SSDM2023-107460

EFFECTS OF MANUFACTURING PROCESSES ON PROGRESSIVE DAMAGE OF COMPOSITES

Sai Krishna Meka¹, Ryan Enos¹, Dianyun Zhang^{1,*}

¹Purdue University, West Lafayette, IN

ABSTRACT

The manufacturing processes of composites involve complex and inter-related procedures that span across multiple physics domains and scales. To understand the effects of the manufacturing processes on a composite laminate we perform a progressive damage analysis on the composite. We aim to compare residual stresses that are developed due to the Cure Hardening Instantaneous Linear Elastic (CHILE) model, and residual stresses developed due to a simple temperature drop from the rubbery state to glassy state during the manufacturing of the composite. On the application of mechanical loading after the curing of the composite, we incorporate the smeared crack approach to account for the progressive damage of the composite.

Keywords: Cure Kinetics, CHILE, Smeared Crack Approach,

NOMENCLATURE

 G_{23}

 ν_{12}

 ν_{23}

D	Continuum Sunness [m L 1]
\mathbf{D}^{cr}	Unloading Stiffness $[ML^{-1}T^{-2}]$
\mathbf{D}^{da}	Damping matrix $[ML^{-1}T^{-1}]$
N	Transformation Matrix
e^{cr}	Crack strain in crack coordinate system
s^{cr}	Crack stress in crack coordinate system
L	Characteristic Length [L]
σ	Total Stress $[ML^{-1}T^{-2}]$
$oldsymbol{arepsilon}$	Total strain
$arepsilon^{co}$	Continuum strain
$arepsilon^{cr}$	Crack strain
$arepsilon^{el}$	Elastic strain
$arepsilon^{pl}$	Plastic strain
$arepsilon_{nn}^{cr}$	local critical strain in the normal direction
E_1	Longitudinal Elastic modulus $[ML^{-1}T^{-2}]$
E_2	Transverse Elastic modulus $[ML^{-1}T^{-2}]$
G_{12}	Shear12 modulus $[ML^{-1}T^{-2}]$

Continuum Stiffness [$ML^{-1}T^{-2}$]

Poisson's ratio 12

Poisson's ratio 23

Shear23 modulus $[ML^{-1}T^{-2}]$

1. INTRODUCTION

Fiber reinforced composites are used extensively in the aerospace field, transportation sector, automotive industry to prepare structural components because of their lightweight and relatively high strength characteristics. The manufacturing of these composites takes place at high temperature to ensure complete curing of the resin in the composite system. The characterization of such fiber reinforced composites requires the use of cure kinetics models to describe the state of cure within the resin after the composite system has been subjected to a thermal history.

No composite material is free from residual stresses. Residual stresses are self-equilibrating stresses in materials without external loading. So, even before a mechanical load is applied on the composite, the system has inherent stresses. In composites one of the main reasons for the development of the residual stresses is the difference in the values of the thermal expansion coefficients of the fiber system and the matrix system. As the composite system undergoes curing the resin changes its state based on the curing cycle that the composite is subjected to during the manufacturing process. As the resin keeps changing its state during the course of manufacturing, the thermal properties of the resin also change. Due to this, the residual stresses that are developed in the composite system evolves with time depending on the cure kinetics of the resin system.

The knowledge about the residual stresses developed in the material system is important because without that information we would over-predict the capabilities of a composite material. In many applications this might be very dangerous and may have a severe impact. We try to address this problem by calculating the residual stresses developed in the system due to the manufacturing processes and develop constitutive models that calculate incremental stresses and strains. With the help of an incremental formulation we can calculate stresses and strains in a system that do not necessarily begin experiencing stresses from a relaxed state.

However, it is computationally costly and also difficult to identify an appropriate cure kinetics model to predict the residual stress that is developed based on the curing cycle used for manufacturing. Instead we explore the possibility of using only

^{*}Corresponding author: dianyun@purdue.edu

the temperature dropping part of the cure cycle where the resin is in its glassy state, to obtain the residual stresses that develop at the end of the temperature drop. It is observed that the residual stresses developed in both the cases are very similar.

After the composite is manufactured we also see that there are micro-cracks that form in the material system. The presence of these micro-cracks needs to be accounted for as these micro-cracks grow when there is a load applied on the system. The micro-cracks grow in size and may coalesce with other micro-cracks damaging the material. When the micro-cracks grow in size and coalesce with one another it would lead to formation of macro-crack leading to failure of the material. Using the smeared crack approach, in which the effects of a crack are smeared across the element. This is developed using the ideas of continuum damage mechanics we formulate a constitutive model for the material to understand the stress-strain response of the system.

Here in this paper we aim to combine the effect of development of residual stresses with the smeared crack approach to predict the stress-strain response of a composite material system. We try to suggest an alternate way to calculate the residual stresses developed due to the manufacturing process instead of using the CHILE (Cure Hardening Instantaneous Linear Elastic) model and compare its results with the CHILE model results.

2. MULTI PHYSICS MODEL OF COMPOSITE CURING PROCESS

The curing process in the composite processing model involves multiple physical phenomena such as resin cure kinetics, chemical shrinkage, and thermal loading. In order to predict curing induces residual stresses we employ the modeling framework developed in [1]. According to [1] for an epoxy resin such as EPON 862/W, the cure kinetics relation can be expressed using the Kamal-Souror autocatalytic model as

$$\frac{d\phi}{dt} = \left(A_1 exp\left(-\frac{\triangle E_1}{RT}\right) + A_2 exp\left(-\frac{\triangle E_2}{RT}\right)\phi^m\right)(1-\phi)^n.$$

Where $\triangle E_1$ and $\triangle E_2$ are the activation energies, R=8.314 J/mol/K is the universal gas constant, and A_1 , A_2 , m, and n are the cure kinetics parameters. These cure kinetics parameters can be determined by measuring the resing heat generation response under various temperatures using a Differential Scanning Calorimeter. Here, we use the values of these properties as specified in [1] mentioned in table 1

The simplified cure-dependent composite constitutive relation from [1] is

$$\Delta \sigma = C_i (\Delta \varepsilon - \Delta \varepsilon^{th} - \Delta \varepsilon^{ch}).$$

Where σ is the stress tensor, C_i is the composite relaxation stiffness tensor where i=R, G represent the composite properties at the rubbery and glassy phases, respectively, $\Delta \varepsilon$, $\Delta \varepsilon^{th}$, and $\Delta \varepsilon^{ch}$ are the increments in total, thermal, and chemical strains respectively. We have to note that the thermal strains are developed due to the temperature change during curing, which is expressed as $\Delta \varepsilon^{th} = \alpha \Delta T$. Where α is the temperature and curedependent Coefficient of Thermal Expansion (CTE). The value

TABLE 1: PARAMETERS USED IN THE CURE KINETICS MODEL FOR THE EPON 862/W SYSTEM

Cure kinetics parameter	Characterized value	Value from literature	Unit
A_1	0	0	1/s
$\triangle E_1$	-	-	J/mol
A_2	7098	6488	1/s
$\triangle E_2$	5.5E+04	5.3E+04	J/mol
m	0.40	0.39	-
n	1.65	1.67	-
H_r	406.12	399.00	J/g

of α is different in the rubbery and glassy state, therefor based on the curing temperature we need to account for the value of α accordingly. As the degree of cure (DOC) progresses from 0 to 1. The chemical strains that develop in the resin are ascribed to the volumetric shrinkage due to resin cross-linking. This cross-linking can be assumed to be proportional to the DOC [2]. The total chemical shrinkage, v_{sh}^T , can be measured using various techniques as discussed in [1]. The effective volume shrinkage is found using

$$\varepsilon_V = v_{sh}^T (1 - \phi_{gel}).$$

The effective volume shrinkage is then used to compute the effective shrinkage strain using

$$\varepsilon_m^{ch} = (\varepsilon_V + 1)^{1/3} - 1.$$

Where the ϕ_{gel} is the DOC at gelation point. Considering that ε_m^{ch} represents the resin strain accumulated as the state of resin progressed from the gelation point, this property can be treated in the same way as CTE. Thus, the coefficient of chemical shrinkage (β_m) for the resin is defined as

$$\beta_m = \frac{\varepsilon_m^{ch}}{1 - \phi_{gel}}.$$

The thermo-chemo-mechanical properties of the EPON 862/W system are listed in table 2.

The curing process in a thermoset resin can be divided into three regions as shown in figure 1. Gelation occurs at a defined point in the curing reaction, after which the resin is able to carry loads. Before this point (Region A), the resin is in the liquid phase and stress accumulation is negligible. After gelation, the resin transitions to the solid phase and the thermal and chemical strains (ϵ^{th} and ϵ^{ch}) should be considered in the constitutive relations. When the curing temperature is above the resin glass transition temperature (Region B), the resin is at a rubbery state and it is assumed that the resin modulus is close to zero, and its poisson's ratio is close to 0.5 since a gel can be approximated as an incompressible material.

Once the glass transition temperature of the resin exceeds the curing temperature, the resin is across the vitrification point and transitions from the rubbery state to the glassy state (Region

TABLE 2: THERMO-CHEMO-MECHANICAL PROPERTIES OF THE EPON 862/W SYSTEM

Symbol	Definition	Value	Unit
ρ_m	Density	1,200	kg/m^3
$C_{p,m}$	Specific Heat	1,150	J/kg/K
k_m	Thermal Conductivity	0.188	W/m/K
α_m^R	CTE at the rubbery state	1.82E-04	1/ <i>K</i>
α_m^G	CTE at the glass state	7.78E-05	1/ <i>K</i>
v_{sh}^T	Chemical shrinkage (volume)	-0.0372	-
E_m^R	Modulus at the rubbery state	32.4E+06	Pa
E_m^G	Modulus at the glassy state	3.24E+09	Pa
v_m^G	Poisson's ratio at the glassy state	0.35	
T_g^0	Glass transition temperature of fully cured resin	246	K
T_g^{∞}	Glass transition temperature of uncured resin	383	K
λ	Fitting parameter	0.39	-
ϕ_{gel}	DOC at gelation	0.71	-

C), followed by an increase in the elastic modulus and decrease in the Poisson's ratio.

The cure and temperature dependent model is implemented in ABAQUS using a user defined subroutine (UMAT). The cure cycle was applied to the surface of the part, starting at room temperature of 25 °C and ramping to the cure temperature of 170 °C in 15 min then holding for 120 min before finally cooling back to room temperature in 45 min. The corresponding cure cycle diagram is as shown in figure 1.

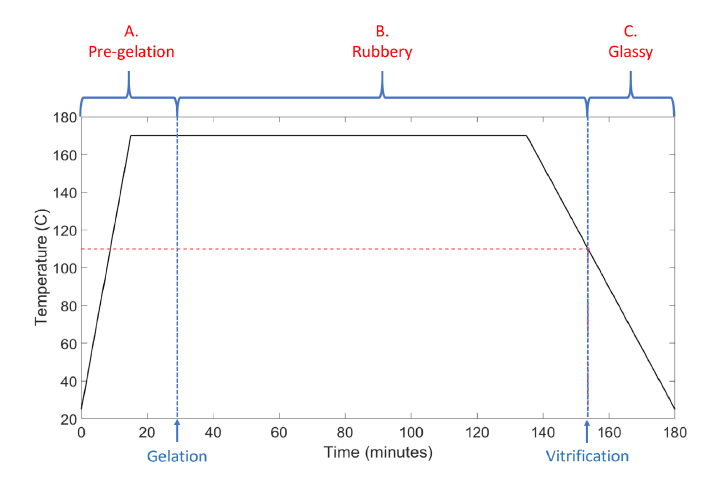


FIGURE 1: CURE CYCLE DIAGRAM

3. SMEARED CRACK APPROACH

To model the progressive damage of composites, the two widely used models are the continuum smeared crack methods (CSCM) and discrete crack methods (DCM). But the computational costs of discrete methods rise as the number of components

to be modeled increases. Therefore, it is impractical to model the response of a large structure with multiple failure mechanisms present in a geometrically nonlinear setting. CSCM are often more efficient compared to DCM, however, the fidelity may be lower. Compared to the explicit modelling of cracks, in the CSCM, the effect of cracks is modeled during progressive failure much more efficiently. To construct the constitutive law for the post-peak behavior of the composite, we adopted the Smeared Crack Approach (SCA). In SCA, the effect of the micro-cracks are smeared over a characteristic length as shown in figure 2. This smearing effect is mathematically characterized by deteriorating the secant stiffness of the material as the damage progresses once the transition criteria (i.e. failure criteria) is satisfied.

The transition criteria used for each of the plies is the maximum stress criteria. When the local stresses reach the critical strength value, we conclude that failure has initiated and the material transitions from pre-peak behavior to post-peak behavior. The pre-peak behavior corresponds to the matrix micro damage due to the growth of voids and flaws in the matrix, while the post-peak behavior corresponds to the accumulation of matrix micro damage which leads to matrix macroscopic cracking [4]. The pre-peak behavior is governed by a linear elastic constitutive law, i.e., a strain-based formulation. While in the post-peak regime the softening of the material is captured by a displacement-based formulation of linear traction-separation law as show in figure 3.

In the pre-peak regime, standard continuum descriptions of the material are assumed to hold. In the post-peak regime, it is assumed that the total strain ε may be split up into a continuum part and a crack part. Therefore, the total strain can be expressed as follows -

$$\varepsilon = \begin{cases} \varepsilon^{co} & \text{in the pre-peak regime} \\ \varepsilon^{co} + \varepsilon^{cr} & \text{in the post-peak regime.} \end{cases}$$

Where, ε^{co} is the continuum strain and ε^{cr} is the crack strain. The continuum strain ε^{co} can further be decomposed into elastic (ε^{el}) and plastic contributions (ε^{pl}) as

$$\varepsilon^{co} = \varepsilon^{el} + \varepsilon^{pl}. \tag{1}$$

In the current formulation, we are not considering any plasticity to be present. Therefore, $\varepsilon^{co} = \varepsilon^{el}$. The relation between the local crack strains and the global crack strains is

$$\varepsilon^{cr} = Ne^{cr} = N \begin{bmatrix} \varepsilon_{nn}^{cr} \\ \gamma_{t1}^{cr} \\ \gamma_{t2}^{cr} \end{bmatrix}. \tag{2}$$

Where 'N' is the transformation matrix. (See Appendix A for the derivation).

Similarly, global stress (σ) can be transformed to yield the tractions at the crack interface (s^{cr}) as follows -

$$s^{cr} = \begin{bmatrix} \sigma_{nn}^{cr} \\ \tau_{t1}^{cr} \\ \tau_{t2}^{cr} \end{bmatrix} = N^T \sigma.$$

The tractions at the crack interface (s^{cr}) are related to the crack strain (e^{cr}) through the secant stiffness matrix (D^{cr}) and a

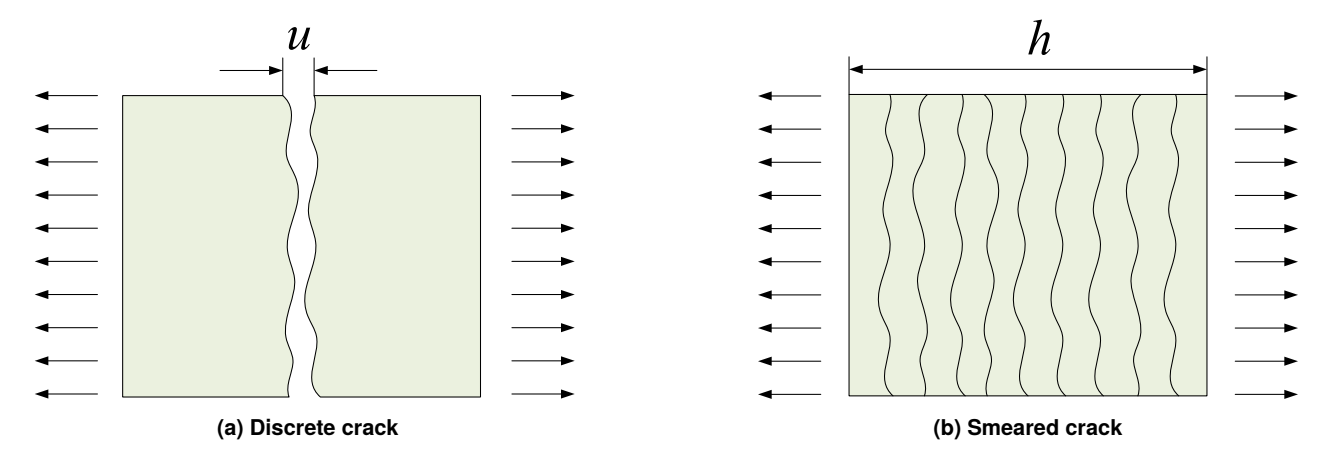


FIGURE 2: DISCRETE CRACKS SMEARED WITHIN A FINITE ELEMENT [3]

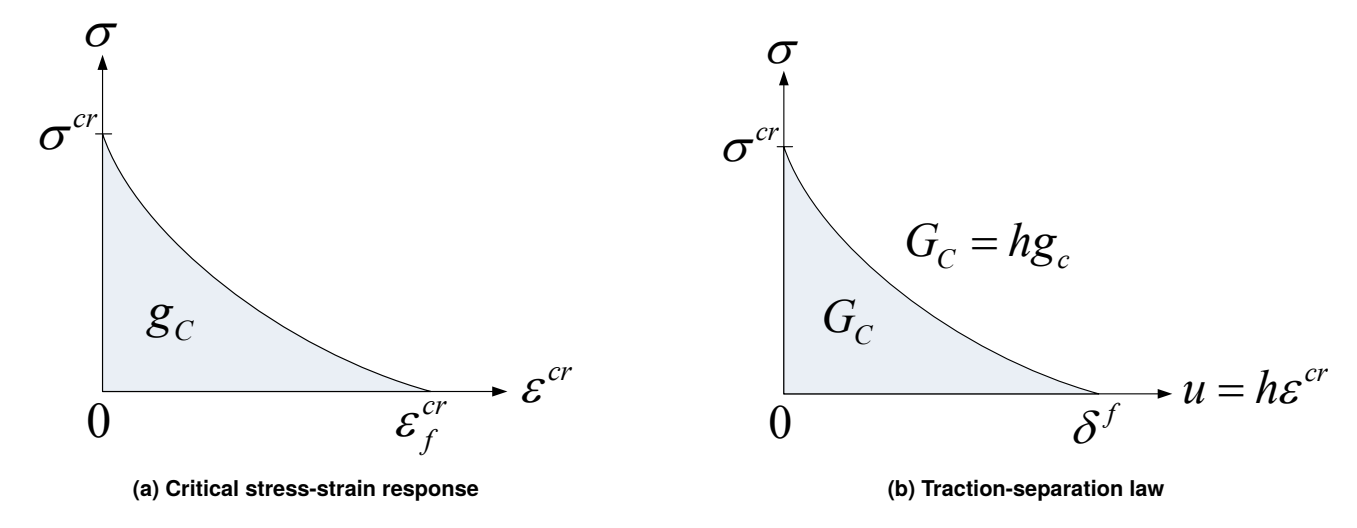


FIGURE 3: STRESS-STRAIN SOFTENING RESPONSE IS RELATED TO THE TRACTION-SEPARATION LAW THROUGH A CHARACTERISTIC LENGTH. [3]

damping matrix (D^{da}) by

$$s^{cr} = D^{cr}e^{cr} + D^{da}\dot{e}^{cr}$$

The damping matrix makes the crack progression a timedependent property. This can also be used to smoothen the numerical solution scheme. Any numerical scheme involves a discrete time step. The crack strain rate is accordingly approximated with finite differences as

$$\dot{\mathbf{e}}^{cr} \approx \frac{e^{cr}(t+\Delta t) - e^{cr}(t)}{\Delta t} = \frac{e^{cr} - e^{cr}_{old}}{\Delta t}.$$

The relation between the total stiffness (global) i.e. " σ " and the elastic strain i.e. " ε " is

$$\sigma = D^{co} \varepsilon^{el}$$
.

Where D^{co} is the continuum stiffness matrix, given by $(S^{co})^{-1}$ and S^{co} is compliance matrix given as follows for a transversely

isotropic material:

$$S^{co} = \begin{bmatrix} \frac{1}{E_1} & \frac{-\nu_{12}}{E_1} & \frac{-\nu_{12}}{E_1} & 0 & 0 & 0 \\ -\frac{\nu_{12}}{E_1} & \frac{1}{E_2} & -\frac{\nu_{23}}{E_2} & 0 & 0 & 0 \\ -\frac{\nu_{12}}{E_1} & -\frac{\nu_{23}}{E_2} & \frac{1}{E_2} & 0 & 0 & 0 \\ 0 & 0 & 0 & \frac{1}{G_{12}} & 0 & 0 \\ 0 & 0 & 0 & 0 & \frac{1}{G_{12}} & 0 \\ 0 & 0 & 0 & 0 & 0 & \frac{2(1+\nu_{23})}{E_2} \end{bmatrix}$$

Note:
$$G_{23} = \frac{E_2}{2(1 + \nu_{23})}$$

Combining all equations results in an implicit relation between the crack strain and the total elastic strain.

$$e^{cr} = \left[D^{cr}(e^{cr}) + N^T D^{co} N + \frac{1}{\Delta t} D^{da}\right]^{-1} \left[N^T D^{co} \varepsilon^{cr} + \frac{1}{\Delta t} D^{da} e^{cr}_{old}\right]$$
(3)

Finally, the relation between total stress and total strain in the post-peak regime is formulated as

$$\sigma = \left[D^{co} - D^{co} N \left(D^{cr} + N^T D^{co} N + \frac{1}{\Delta t} D^{da} \right)^{-1} N^T D^{co} \right] \varepsilon^{cr}$$
$$- \frac{1}{\Delta t} \left[D^{cr} (e^{cr}) + N^T D^{co} N + \frac{1}{\Delta t} D^{da} \right]^{-1} D^{da} e^{cr}_{old} \quad (4)$$

The *total* stress-strain equation 4, which is more suited large time increments during reversed loading, and when there are no pre-defined stress fields on the system. Equation 3 is a highly non-linear equation for the crack strain. It is solved via Newton's method by defining a function that is to be minimized [5].

4. CONSTITUTIVE MODEL

The stress-strain response of the model has to be split into two parts. The first part being "During Curing" and the second part being "Post-Curing". During curing the system follows the stress strain response as governed by the constitutive relation established in equation 2.

4.1 During Curing

We consider two cases for the "During Curing" stage, one case where we use the auto-catalytic cure kinetics model which considers the effect of the shrinkage strains and the the thermal strains that are developed during the rubbery state and glassy state. The other case being a simple temperature drop from the vitrification point to the room temperature at which the composite material will be brought to after curing.

In the case of a simple temperature drop we do not account for the residual stresses that are developed till the vitrification point, simply put we assume that the resin is stress free at the vitrification point and let the residual stressed develop as the temperature drops to room temperature.

The temperature drop profile diagram is as shown in figure 4

4.1.1 Cure Kinetics. In the pre-gelation stage the resin is in the liquid state and there are no stresses developed. As the gelation point occurs in the cure cycle the resin becomes rubbery and the Young's modulus of the resin changes to E_m^R and the thermal expansion coefficient of the resin is α_m^R . The constitutive relation during the rubbery state is hence given as

$$\Delta \sigma = C_R (\Delta \varepsilon - \alpha_m^R \Delta T - \Delta \varepsilon^{ch})$$

Where C_R is the stiffness matrix calculated for the isotropic matrix whose Young's Modulus is E_m^R and poisson's ratio is ν_R (for this particular material it so happens that the poisson's ratio

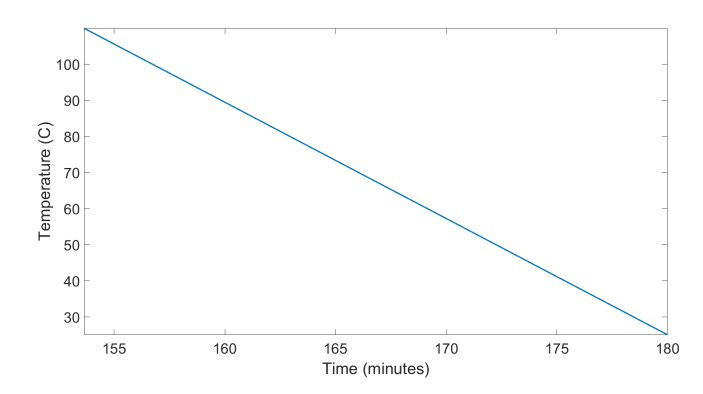


FIGURE 4: GLASSY STAGE OF CURE CYCLE DIAGRAM

in both the rubbery and glassy state are almost the same. Hence $v^R = v^G$)

Similary, in the Glassy state the constitutive law modifies to

$$\Delta \sigma = C_G(\Delta \varepsilon - \alpha_m^G \Delta T - \Delta \varepsilon^{ch}).$$

Where C_G is the stiffness matrix calculated for the isotropic matrix whose Young's Modulus is E_m^G and poisson's ratio is v_G

4.1.2 Temperature Drop. In the case of a simple temperature drop the constitutive law modifies to

$$\Delta \sigma = C_G (\Delta \varepsilon - \alpha_m^G \Delta T) \tag{5}$$

as the shrinkage is no longer considered.

4.2 Post-Curing

As stated earlier, in order to use the ideas of the smeared crack approach when there are pre-defined stresses developed in the material system, we need to resort to an incremental formulation of SCA. The incremental formulation is done by tweaking the total form equations that were developed earlier.

The equation 3 modifies to 6

$$\Delta \sigma = D^{co} \Delta \varepsilon \tag{6}$$

Similary equations 1 and 2 are modified to

$$\triangle \varepsilon = \triangle \varepsilon^{co} + \triangle \varepsilon^{cr}$$

$$\triangle \varepsilon^{cr} = \triangle N e^{cr}.$$

However, the relationship between the crack stress and the global stress is the same as it was in the total form. Similarly, the relationship between the local crack stress and the local crack strain is also the same as it was in total form, which is

$$s^{cr} = N^T \sigma$$

$$s^{cr} = D^{cr} \rho^{cr} + D^{da} \dot{\rho}^{cr}$$

By definition of incremental strain and incremental stress the following equations 7 and 8 are written.

$$e^{cr} = e^{cr}_{old} + \Delta e^{cr} \tag{7}$$

$$\sigma = \sigma_{old} + \Delta \sigma \tag{8}$$

Then following equation 3 we arrive at equation 9 and we solve for e^{cr} .

$$\left(N^T D^{co} N + D^{cr} + \frac{D^{da}}{\Delta t}\right) e^{cr} - N^T D^{co} \Delta \varepsilon$$

$$- \frac{D^{da}}{\Delta t} e^{cr}_{old} - N^T D^{co} N e^{cr}_{old} - N^T \sigma_{old} = 0 \quad (9)$$

This is then used to update the stress as follows

$$\sigma = \sigma_{old} + D^{co}(\Delta \varepsilon - N(e^{cr} - e^{cr}_{old}))$$

5. DISCRETE RVE MODEL

We generate a discrete 3D RVE model in which the fibers are cylindrical and are randomly dispersed in the matrix with a interphase material between the fiber and matrix, with a fixed value of volume fraction as shown in figure 5. This discrete RVE is subjected to curing as well as temperature drop (cooling) with the temperature vs time profiles as shown in 1 and 4 respectively.

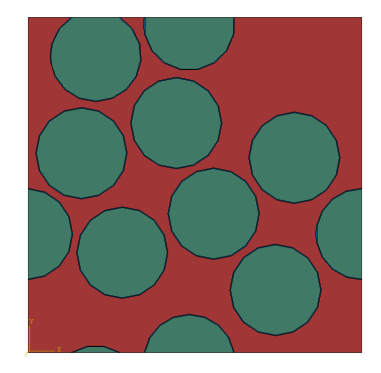


FIGURE 5: DISCRETE RVE MODEL

We look at the residual stresses that are developed in the matrix system after it is subjected to curing and simple cooling. Based on the observation of the stresses that are developed we propose the use of simple cooling as an alternate to the usage of CHILE model.

6. RESULTS AND DISCUSSION

The stressed developed in the discrete RVE due to the curing and the temperature drop are as shown in 7 and 6 respectively. It can be seen that the magnitude of the maximum stress that is developed is just slightly higher in the case of the simple temperature drop model when compared to the cure kinetics model, as there is no shrinkage that is accounted for in the temperature drop model. The locations where the maximum stresses are developed are also almost same in both the models. Hence it is sufficient to show that if we apply a mechanical loading on the model that has undergone just cooling in the glassy state it's stress-strain response would be very close to a mechanically loaded cured model that had CHILE incorporated in it.

Now upon applying a mechanical loading on the cooled discrete RVE and activating the smeared crack incremental formulation by using a user defined subroutine (UMAT) we get the stress vs strain on the RVE as shown in figure 8.

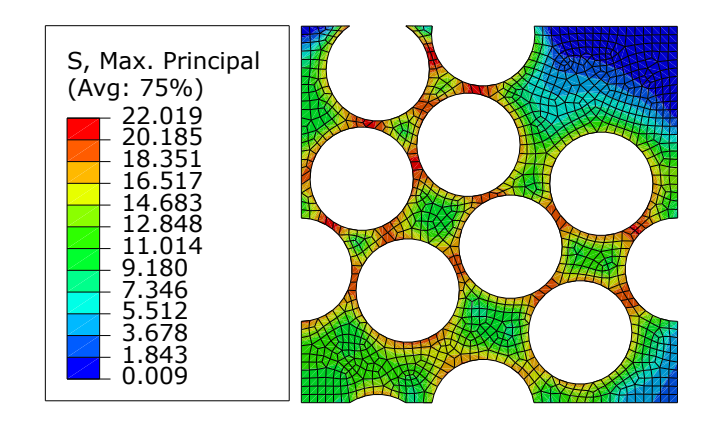


FIGURE 6: PRINCIPAL STRESS CONTOUR PLOT FOR RVE MODEL UNDERGOING COOLING

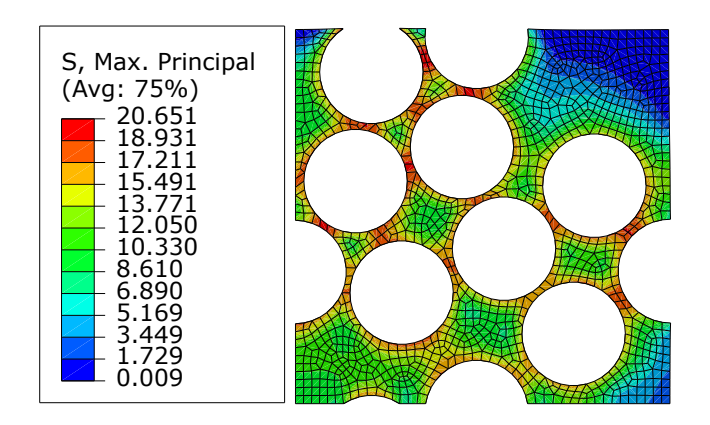


FIGURE 7: PRINCIPAL STRESS CONTOUR PLOT FOR RVE MODEL UNDERGOING CURING

The locations of elements where the crack had occurred and have locally failed are as shown in the figure 9 (elements in red color have failed).

An interesting point to note is that although the SCA has the ability to capture the material strain softening behavior, it is pathologically mesh dpendent since no characteristic length scale is associated with the damage evolution. Upon increasing the mesh size by a factor of two it is observed that the locations of the elements which have cracked had changed significantly as shown in figure 10. The element size to thickness of the RVE ration in the model with smaller mesh is around 0.8 while the ratio in the model with bigger mesh is around 1.6.

7. CONCLUSION

The usage of simple temperature drop model as an alternate to the CHILE model is explored. Even though the residual stresses that are developed are slightly overpredicted compared to that of the stresses developed in a model in which CHILE is incorporated the difference is not very significant. This helps us with the task of finding an appropriate cure kinetics model for the curing cycle and the material system and developing a UMAT. To predict the progressive damage of the model we need to keep an eye on the mesh size and how the variation of mesh size is leading to the change in the positions of the elements where the

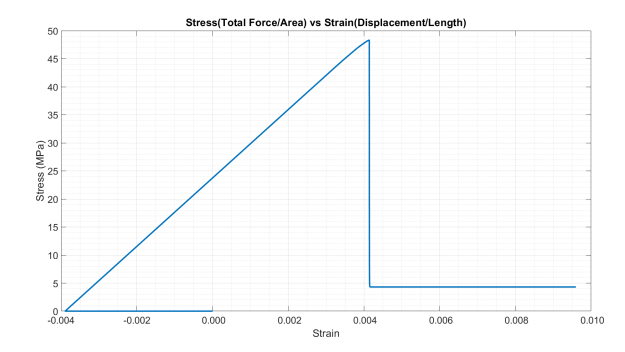


FIGURE 8: STRESS VS STRAIN BEHAVIOUR ON A MECHANICALLY LOADED DISCRETE RVE AFTER BEING COOLED

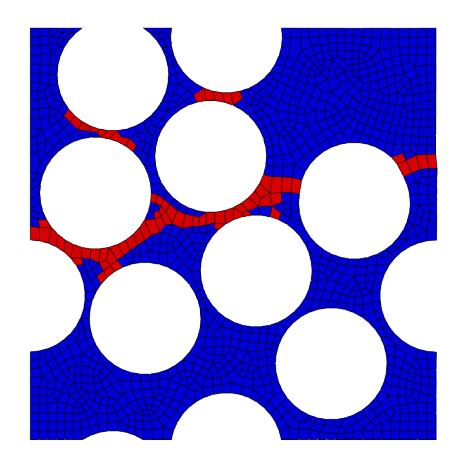


FIGURE 9: CRACKED ELEMENTS IN DISCRETE RVE MODEL

crack is developing. As long as we are choosing a small enough element size within the Bazant limit and there is no change in the crack locations with the change in mesh size we should be fine with the choice of mesh size.

ACKNOWLEDGMENTS

We thank Haotian Sun (University of Connecticut) for helping us develop the preliminary code for the incremental Smeared Crack Approach and for many fruitful discussions that lead to enhancement and betterment of the user defined subroutine code.

REFERENCES

- [1] Zhou, Kai, Enos, Ryan, Zhang, Dianyun and Tang, Jiong. "Uncertainty analysis of curing-induced dimensional variability of composite structures utilizing physics-guided Gaussian process meta-modeling." *Composite Structures* Vol. 280 (2022): p. 114816.
- [2] Bogetti, Travis A and Gillespie Jr, John W. "Process-induced stress and deformation in thick-section thermoset composite laminates." *Journal of composite materials* Vol. 26 No. 5 (1992): pp. 626–660.
- [3] Zhang, Dianyun, Waas, Anthony M. and Yen, Chian-Fong. "Progressive damage and failure response of hybrid 3D textile composites subjected to flexural loading, part II: Mechanics based multiscale computational modeling of progressive

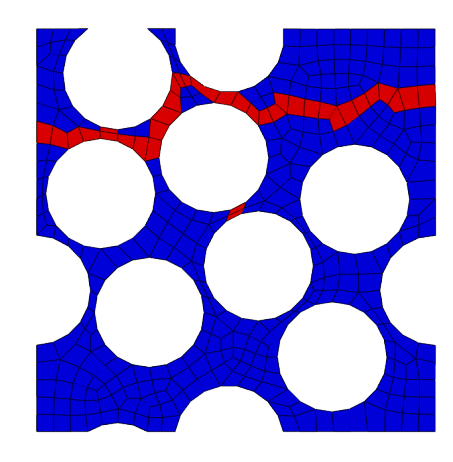


FIGURE 10: CRACKED ELEMENTS IN DISCRETE RVE MODEL

- damage and failure." *International Journal of Solids and Structures* Vol. 75-76 (2015): pp. 321–335.
- [4] Bažant, Zdeněk P and Oh, Byung H. "Crack band theory for fracture of concrete." *Matériaux et construction* Vol. 16 No. 3 (1983): pp. 155–177.
- [5] Heinrich, Christian and Waas, Anthony. "Investigation of progressive damage and fracture in laminated composites using the smeared crack approach."

APPENDIX A. CALCULATING THE TRANSFORMATION MATRIX (N)

'N' is dependent on the crack plane orientation and the derivation of it is as follows:

$$x_i' = a_{ip} x_p \tag{10}$$

where $a'_{ij}s$ are the direction cosines governing the space vector transformation between crack coordinates and global coordinates. So the stress transformation is as follows:

$$\sigma'_{ij} = a_{ip}a_{jq}\sigma_{pq} \tag{11}$$

i.e. in the matrix form given as:

$$\begin{pmatrix}
\sigma'_{11} \\
\sigma'_{22} \\
\sigma'_{33} \\
\sigma'_{12} \\
\sigma'_{13} \\
\sigma'_{23}
\end{pmatrix} = \begin{bmatrix}
K1 & 2K2 \\
K3 & K4
\end{bmatrix} \begin{pmatrix}
\sigma_{11} \\
\sigma_{22} \\
\sigma_{33} \\
\sigma_{12} \\
\sigma_{13} \\
\sigma_{23}
\end{pmatrix}$$
(12)

Where,

$$\mathbf{K_1} = \begin{bmatrix} a_{11}^2 & a_{12}^2 & a_{13}^2 \\ a_{21}^2 & a_{22}^2 & a_{23}^2 \\ a_{31}^2 & a_{32}^2 & a_{33}^2 \end{bmatrix}$$
(13)

$$\mathbf{K_2} = \begin{bmatrix} a_{11}a_{12} & a_{11}a_{13} & a_{12}a_{13} \\ a_{21}a_{22} & a_{21}a_{23} & a_{22}a_{23} \\ a_{31}a_{32} & a_{31}a_{33} & a_{32}a_{33} \end{bmatrix}$$
(14)

$$\mathbf{K_3} = \begin{bmatrix} a_{11}a_{21} & a_{12}a_{22} & a_{13}a_{23} \\ a_{11}a_{31} & a_{12}a_{32} & a_{13}a_{33} \\ a_{21}a_{31} & a_{22}a_{32} & a_{23}a_{33} \end{bmatrix}$$
(15)

$$\mathbf{K_4} = \begin{bmatrix} a_{11}a_{22} + a_{12}a_{21} & a_{11}a_{23} + a_{13}a_{21} & a_{12}a_{23} + a_{13}a_{22} \\ a_{11}a_{32} + a_{12}a_{31} & a_{11}a_{33} + a_{13}a_{31} & a_{12}a_{33} + a_{13}a_{32} \\ a_{21}a_{32} + a_{22}a_{31} & a_{21}a_{33} + a_{23}a_{31} & a_{22}a_{33} + a_{23}a_{32} \end{bmatrix}$$

Therefore, if the global co-ordinates are the 1-2-3 coordinates, while local crack orients in the 1'-2'-3' coordinate system with the crack normal aligned in that 1'-direction

$$\begin{pmatrix}
\epsilon_{11} \\
\epsilon_{22} \\
\epsilon_{33} \\
\gamma_{12} \\
\gamma_{13} \\
\gamma_{23}
\end{pmatrix} = \begin{bmatrix} N \end{bmatrix} \begin{Bmatrix}
\epsilon'_{11} \\
\gamma'_{12} \\
\gamma'_{13} \\
\gamma'_{13}
\end{Bmatrix}$$
(17)

$$\begin{cases}
\sigma'_{11} \\ \sigma'_{12} \\ \sigma'_{13}
\end{cases} = \begin{bmatrix} N^T \end{bmatrix} \begin{cases}
\sigma_{11} \\ \sigma_{22} \\ \sigma_{33} \\ \sigma_{12} \\ \sigma_{13} \\ \sigma_{23}
\end{cases}$$
(18)

When the 1 direction coincides with 1' direction we have 'N' as follows:

$$\mathbf{N} = \begin{bmatrix} a_{11}^2 & a_{11}a_{21} & a_{11}a_{31} \\ a_{12}^2 & a_{12}a_{22} & a_{12}a_{32} \\ a_{13}^2 & a_{13}a_{23} & a_{13}a_{33} \\ 2a_{11}a_{12} & a_{11}a_{22} + a_{12}a_{21} & a_{11}a_{32} + a_{12}a_{31} \\ 2a_{11}a_{13} & a_{11}a_{23} + a_{13}a_{21} & a_{11}a_{33} + a_{13}a_{31} \\ 2a_{12}a_{13} & a_{12}a_{23} + a_{13}a_{22} & a_{12}a_{33} + a_{13}a_{32} \end{bmatrix}$$
 (19)